Acta Crystallographica Section D
Biological Crystallography
ISSN 0907-4449

Structure of the N-terminal domain of human FKBP52

Pengyun Li,[a] Yi Ding,[a] Beili Wu,[a] Cuiling Shu,[b] Beifen Shen[b] and Zihe Rao[a]*

[a]MOE Laboratory of Protein Science and Laboratory of Structural Biology, Department of Biological Science and Biotechnology, Tsinghua University, Beijing 100084, People's Republic of China, and [b]Beijing Institute of Basic Medical Science, Beijing 100850, People's Republic of China

Correspondence e-mail: raozh@xtal.tsinghua.edu.cn

Received 26 June 2002
Accepted 24 September 2002

PDB Reference: FKBP52, 1n1a.

FKBP52 is a member of the FK506-binding protein family (FKBPs). The N-terminal domain of FKBP52 (FKBP52-N; residues 1–140) is responsible for peptidyl–prolyl isomerase activity and binding of FK506. Here, the crystal structure of FKBP52-N has been determined by molecular replacement to 2.4 Å. FKBP52-N is defined by a six-stranded antiparallel β-sheet wrapping with a right-handed twist around a short α-helix, an architecture similar to that of FKBP12. FKBP52-N is able to bind FK506 in a similar way to FKBP12. The variability in two loop regions (residues 70–76 and 108–127) is the principal reason for the specificity differences between FKBP52-N and FKBP12. The Pro120 change corresponding to Gly89 in FKBP12 limits the conformational adaptation between the loop (residues 108–127) and FK506 and decreases the FK506 affinity, while the Lys121 substitution corresponding to Ile90 of FKBP12 destroys a key interaction between FKBP52-N and calcineurin. It can be inferred from the locations of strictly conserved amino acids in the polypeptide chain that the maintenance of the overall conformation of the PPIase domains of FKBPs is essential for the PPIase activity. The N-terminal region and β-sheets of FKBP52-N forms a hydrophobic patch which may be responsible for the binding of target proteins such as dynein or PAHX.

1. Introduction

Immunophilins are proteins possessing peptidyl–prolyl isomerase (PPIase) domains that bind immunosuppressant drugs. According to their binding affinity for different drugs, immunophilins have been divided into two families: FK506-binding proteins (FKBPs), which bind FK506 and rapamycin, and cyclophilins, which bind cyclosporin A (Dolinski *et al.*, 1997; Galat, 1993).

Several members of the FKBP family have been identified with molecular size ranging from 12 to 65 kDa (Kay, 1996). The best characterized FKBP protein is FKBP12. When complexed with FK506, a macrolide immunosuppressive drug, FKBP12 inhibits the phosphatase activity of calcineurin, modulates Ca^{2+} flux and consequently affects many of the signal transduction pathways responsible for T-cell proliferation and calcium-channel control (Cameron *et al.*, 1995; Griffith *et al.*, 1995; Kissinger *et al.*, 1995; Stoddard & Flick, 1996).

FKBP52 is an immunophilin belonging to the FKBP family, with a molecular weight of 52 kDa, and was first discovered as a component of an untransformed steroid receptor/HSP90 heterocomplex (Sanchez, 1990). Sequence and hydrophobic

cluster analysis suggested FKBP52 to be composed of four different domains, each separated by short hydrophilic linker sequences (Callebaut *et al.*, 1992). Two of these domains are structurally related to FKBP12. The first domain (residues 1–148, defined as FKBP52-I) exhibits 49% sequence identity with FKBP12. This domain is responsible for the PPIase activity of FKBP52 and is able to bind FK506 (Chambraud *et al.*, 1993; Pirkl *et al.*, 2001; Tai *et al.*, 1993; Yem *et al.*, 1992). The second domain (residues 149–253) exhibits 28% sequence identity with FKBP12. There is minimal PPIase activity in this domain (Chambraud *et al.*, 1993; Pirkl *et al.*, 2001). The third domain (residues 264–400) includes three tetratricopeptide repeats (TPRs), which are involved in the binding to HSP90 (Owens-Grillo *et al.*, 1996; Pratt *et al.*, 1999; Ramsey *et al.*, 2000; Silverstein *et al.*, 1997, 1999; Young *et al.*, 1998). The fourth domain (residues 400–458) contains a calmodulin-binding site (Callebaut *et al.*, 1992; Massol *et al.*, 1992).

Although the association between FK506 and FKBP52 is mediated through the FKBP52-I domain, when this complex is formed it is not able to inhibit the phosphatase activity of calcineurin (Lebeau *et al.*, 1994; Wiederrecht *et al.*, 1992). FKBP52 also interacts with cytoplasmic dynein and phytanoyl-CoA α-hydroxylase (PAHX; a peroxisomal enzyme involved in Refsum's disease, peripheral neuropathy, retinitis pigmentosa and cerebellar ataxia) through the FKBP52-I domain. FK506 competes for the binding of FAP48 but does not affect the binding of dynein and PAHX. Consequently, it has been suggested that dynein and PAHX interact with the FKBP52-I domain through sites different from the FK506-binding site. FKBP12 does not interact with dynein or PAHX (Chambraud *et al.*, 1996, 1999; Galigniana *et al.*, 2001; Silverstein *et al.*, 1999).

Despite the homology with FKBP12, the FKBP52-I domain is functionally distinct from FKBP12. The NMR structure of FKBP52-I domain was determined in 1996 (Craescu *et al.*, 1996), but a clear picture of the structure–function relationships requires further structural investigation. In this paper, we characterize the three-dimensional structure of FKBP52-N (FKBP52-I truncated C-terminal hydrophilic hinge, residues 1–140) using X-ray diffraction. Based on the X-ray structure, the structure–function relationships are discussed.

2. Materials and methods

2.1. Protein expression and purification

The coding sequence for human FKBP52-N was cloned into *Escherichia coli* expression vector pET28a(+) (Novagen Inc.). The 6×His-tagged protein was expressed in *E. coli* strain BL21 (DE3) plysE and purified using Ni^{2+}–NTA agarose (Qiagen). The purified protein was shown to be greater than 95% pure by SDS–PAGE.

2.2. Crystallization

The purified protein was exchanged into a buffer containing 10 m*M* sodium cacodylate and was concentrated to 20–30 mg ml^{-1}. Crystallization was performed by the hanging-drop vapour-diffusion method. 1 µl of protein solution was mixed with 1 µl of reservoir solution containing 2.0 *M* ammonium sulfate in 0.1 *M* Tris–HCl buffer pH 8.5 and the mixture was equilibrated against 500 µl reservoir solution at 291 K. Clusters of rod-like crystals appeared after 6 d.

Table 1
Data set and refinement statistics.

Values in parentheses are for the highest resolution shell, 2.49–2.40 Å.

Space group	$P2_1$
Unit-cell parameters	
a (Å)	27.8
b (Å)	58.4
c (Å)	70.9
β (°)	98.3
Resolution range (Å)	40–2.4
Unique reflections	8929 (889)
Data redundancy	10.8 (8.4)
Completeness (%)	99.9 (99.9)
$I/\sigma(I)$	17.3 (9.3)
Solvent content (%)	40
$R_{\rm merge}$ (%)	9.5 (29.4)
$R_{\rm work}$ (%)	20.4
$R_{\rm free}$ (%)	28
No. of residues	250
No. of waters	55
Ramachandran core region (%)	87.6
R.m.s. bond length (Å)	0.018
R.m.s. bond angle (Å)	2.3
Average B factors (Å^2)	38.5

2.3. Data collection and processing

The data were collected to 2.4 Å using a 345 mm MAR Research image-plate system mounted on a Rigaku RU-2000 Cu $K\alpha$ rotating-anode generator operated at 48 kV and 98 mA. During data collection, the crystal was maintained at 100 K using a Cryostream (Oxford Cryosystems) in a cryoprotectant prepared by adding 20% glycerol to the mother liquor. The data were processed and scaled with *DENZO* and *SCALEPACK* (Otwinowski & Minor, 1997).

2.4. Structure determination

The asymmetric unit of the crystal contains two molecules with an approximate solvent content of 40%. The structure of FKBP52-N was determined using molecular replacement with the program *AMoRe* (Navaza, 1994), using the known structure of human FKBP12 (PDB code 1fkj) as a search model. The program *O* (Jones *et al.*, 1991) was used for viewing electron-density maps and manual building. *CNS* (Brünger *et al.*, 1998) was used for refinement, with iterative cycles of simulated annealing and individual *B*-factor refinement in the resolution range 40–2.4 Å. No electron density was found for the 15 N-terminal residues of FKBP52-N. The final structure has $R_{\rm work}$ = 20.4% ($R_{\rm free}$ = 28.0%) and consists of residues 16–140 in both molecule *A* and molecule *B* and 55 water molecules. From the Ramachandran plot generated by *PROCHECK* (Laskowski *et al.*, 1993), the final structure has good stereochemistry, with 87.6% of residues in the most favoured region, 11.4% of residues in the additionally allowed region and 1% of residues in the generously allowed region.

The final refinement statistics for the model are given in Table 1.

3. Results and discussion

3.1. Structural overview

The overall structure of the protein is well defined, with the exception of 15 N-terminal residues that are disordered and are not visible in the electron-density map. The protein structure consists of a six-stranded antiparallel β-sheet wrapping with a right-handed twist around a short α-helix (Fig. 1*a*). The β-sheet strands are defined by the following amino acids: β1, 23–24; β2, 33–39; β3, 52–61; β4a, 66–69; β4b, 77–80; β5, 102–107; β6, 128–138, with Richardson topology +1, +3, +1, −3, +1. The α-helix is composed of residues 88–94. There is a large bulge (residues 70–76) in the fourth β-sheet strand, splitting the strand into β4a and β4b. The loop formed by residues 108–127 includes a single-turn 3_{10}-helix. In addition, two classical β-bulges were observed at Phe67 in β4a and Phe135 in strand β6. The β-sheet and α-helix form a hydrophobic pocket corresponding to the FK506-binding pocket of FKBP12. The pocket is also flanked by the large bulge between the fourth strand of the sheet, residues 85–87 which precede the α-helix, and the loop formed by residues 108–127. The side chains of Tyr57, Phe77, Val86, Ile87, Trp90, Phe130 generate a hydrophobic environment in the pocket interior. The overall structure of FKBP52-N is very similar to that of FKBP12, except for an additional short β-strand near the N-terminus of the protein.

There are two molecules (denoted *A* and *B*) per asymmetric unit and they are related by a pseudo-twofold symmetry. The two molecules interact with each other *via* respective hydrophobic surfaces. The solvent-accessible surface area buried by these two molecules is 1701 Å^2 (13% of the total solvent-accessible surface of these two molecules). Our research data (gel filtration and dynamic light scattering; data not shown) and previous articles have shown that FKBP52-N is a dimer in solution, while FKBP12 is a monomer (Rollins *et al.*, 2000; Yem *et al.*, 1993). It seems that the dimer is composed of molecules *A* and *B* and is stabilized by a hydrogen bond (Lys88*B* NZ–Ile49*A* O) and a salt bridge (Lys88*B*–Glu140*A*) (Fig. 1*b*). In FKBP12, Lys and Ile in the corresponding positions are both substituted by Arg, which is unable to form the hydrogen bond and salt bridge (Glu140 is a extra amino acid compared with the FKBP12 sequence). The absence of these interactions may explain why FKBP12 does not form a dimer. The r.m.s. deviation calculated for the main-chain atoms (C, N, O, C$^\alpha$) between the two molecules is 0.42 Å. The most significant differences between the two molecules occur at the N-termini (residues 16–21), which have different orientations (Fig. 3).

Molecule *A* (*A*1) interacts with another symmetry-related molecule *A* (*A*2) through residues 17–22. The N-terminus of molecule *A*1 extends deeply into the hydrophobic pocket of molecule *A*2. The N-terminus of FKBP52-N contains the dipeptide Leu18–Pro19, which is regarded as a natural substrate motif of PPIases *in vivo*, so the interaction between molecules *A*1 and *A*2 provides an insight into how natural substrates may bind to FKBP52-N. There are three hydrogen bonds between the N-terminus of molecule *A*1 and the hydrophobic pocket of molecule *A*2: Leu18 O (*A*1) to Tyr113 OH (*A*2), Leu18 N (*A*1) to Asp68 OD2 (*A*2) and Pro19 O (*A*1) to Ile87 N (*A*2) (Fig. 2*a*). These three hydrogen bonds are conserved in the structure of FKBP12 complexed with FK506 (Fig. 2*b*).

Further differences between the structures of molecule *A* and molecule *B* occur in the interior of the protein. Firstly, the loop region formed by residues 114–125 of molecule *A* is shifted into the interior of the hydrophobic pocket compared with molecule *B*. Secondly, the phenyl group of Phe77 is rotated by about +83° around the C$^\beta$—C$^\gamma$ bond in molecule *A* relative to molecule *B*. Thirdly, the indole ring of Trp90 moves

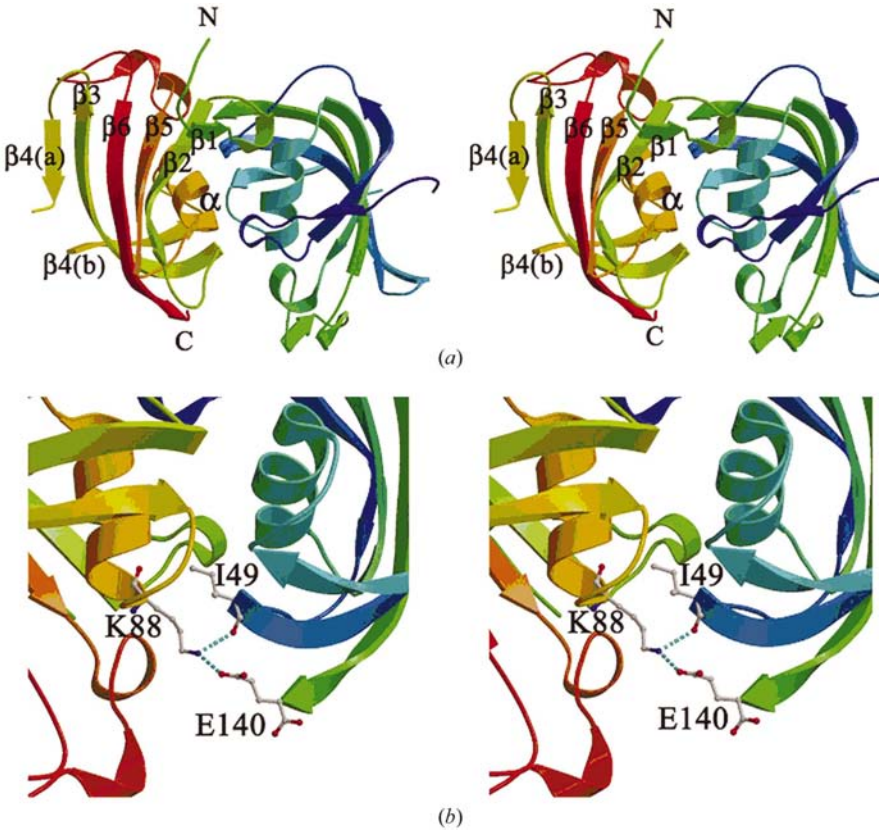

Figure 1
(*a*) Stereoview of the FKBP52-N dimer. (*b*) The hydrogen-bond and salt-bridge interaction between the two monomers. This figure and Figs. 2(*a*), 2(*b*), 3 and 5 were generated using the programs *MOLSCRIPT* (Kraulis, 1991) or *BOBSCRIPT* (Esnouf, 1997).

by 1.4 Å towards the bottom of the pocket in subunit *A*, thus making the binding cavity a little deeper compared with molecule *B*. Similar differences are also observed when the structures of free and complexed FKBP12 are compared. Residues 16–21 of molecule *A* superimpose well with FK506 in the FKBP12–FK506 complex (Fig. 2*c*). We conclude that FK506 binds to FKBP52 by a similar pattern as in its binding to FKBP12 and further suggest that FK506 mimics a transition state of the natural peptidyl–prolyl substrates of FKBPs.

It is possible that molecule *A*1 and molecule *A*2 form a dimer, considering their strong interaction with each other. We have cloned and expressed another recombinant protein including FKBP52-N and the secondary FKBP12-like domain of FKBP52 (residues 1–260), but the gel-filtration profile and dynamic light-scattering results showed it to be a monomer (data not shown). It seems that the secondary FKBP12-like domain can partially occupy the hydrophobic surface of FKBP52-N and prevent two FKBP52-N segments from forming a dimer, which further proves that FKBP52-N forms the dimer *via* hydrophobic surfaces.

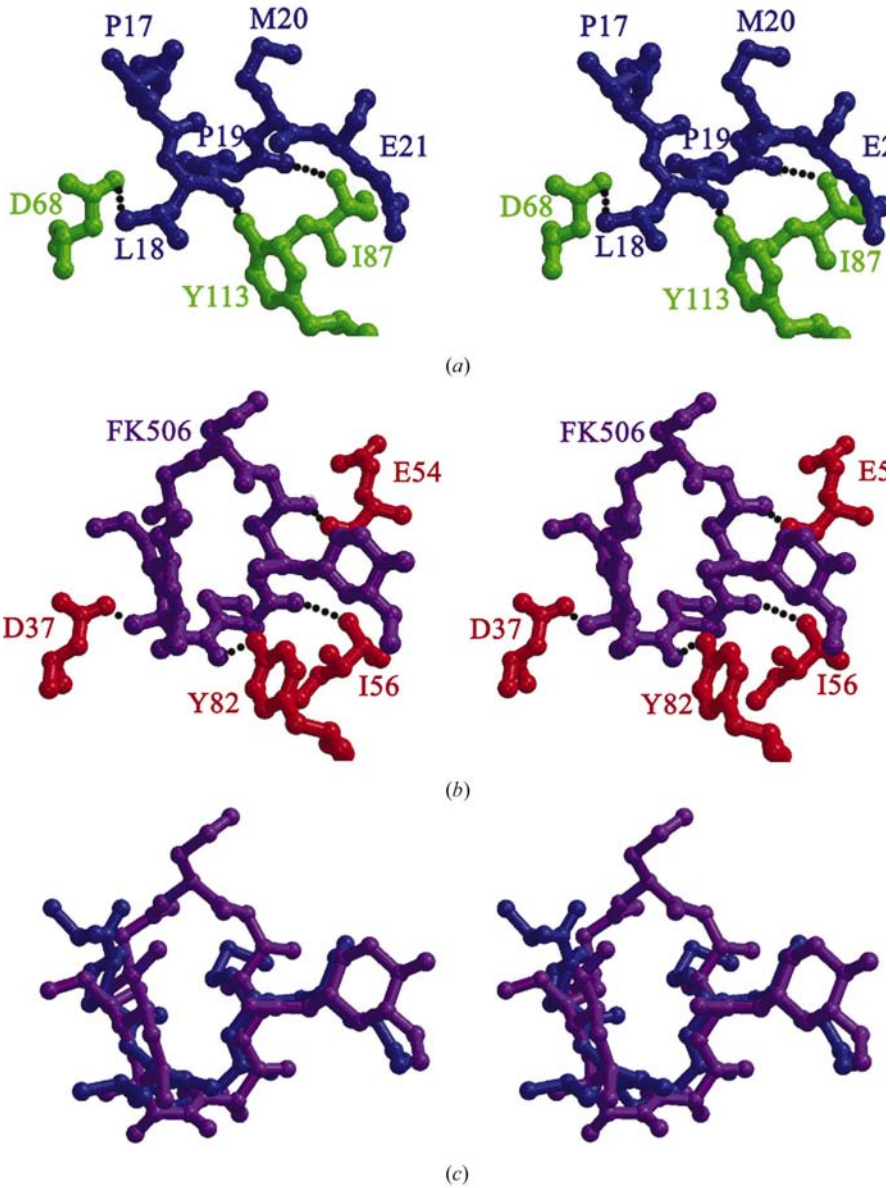

Figure 2
Stereodiagrams illustrating the hydrogen-bond interactions between (*a*) symmetry-related subunits *A*1 and *A*2 in FKBP52-N and (*b*) FK506 and FKBP12. (*c*) Residues 16–21 superimpose well with FK506 in the FKBP12–FK506 complex (FK506, purple; FKBP12 residues, red; molecule *A*2 residues, green; N-terminus of molecule *A*1, blue).

3.2. Comparison with FKBP12

A number of FKBP12 structures have been published, including unliganded and liganded FKBP12. Fig. 3 shows the superposition of FKBP52-N with four FKBP12 structures: unliganded FKBP12 (PDB code 1d6o), FKBP12–FK506 (PDB code 1fkj), FKBP12–rapamycin (PDB code 1fkl) and the FKBP12–FK506–calcineurin complex (PDB code 1tco). The main-chain conformations between these five structures are very similar, except for the loop regions corresponding to residues 41–47, 61–66, 71–76, 81–85 and 117–122. The r.m.s. deviations of all the main-chain atoms (calculated against molecule *A* of FKBP52-N) are 0.8 Å for unliganded FKBP12, 0.9 Å for FKBP12–FK506, 0.8 Å for FKBP12–rapamycin and 0.93 Å for FKBP12–FK506–calcineurin. The largest difference occurs for the region of residues 41–47. In this region, the conformations of both molecule *A* and molecule *B* of FKBP52-N have distinct differences from the corresponding regions of the FKBP12s, with variations of up to 2 Å when the molecules are superimposed. These differences are likely to be responsible for the differences in the substrate specificity of FKBP52-N.

3.3. Functional implications

In FKBP12, the polypeptide segment between Ala84 and Asn94 moves to interact with small ligands (Wilson *et al.*, 1995). In this segment, there are five differences in the amino-acid sequence between FKBP12 and FKBP52: Ala84, Thr85, His87, Gly89 and Ile90 of FKBP12 are changed to Ser115, Ala116, Ser118, Pro120 and Lys121, respectively, in FKBP52-N. These changes, especially Gly to Pro, may restrain the movement of the loop and result in an unfavourable conformation for ligand binding; the G89P mutant of FKBP12 decreases the affinity for FK506 by sevenfold (Craescu *et al.*, 1996). This suggests the FKBP52 affinity for FK506 is much lower than that of FKBP12.

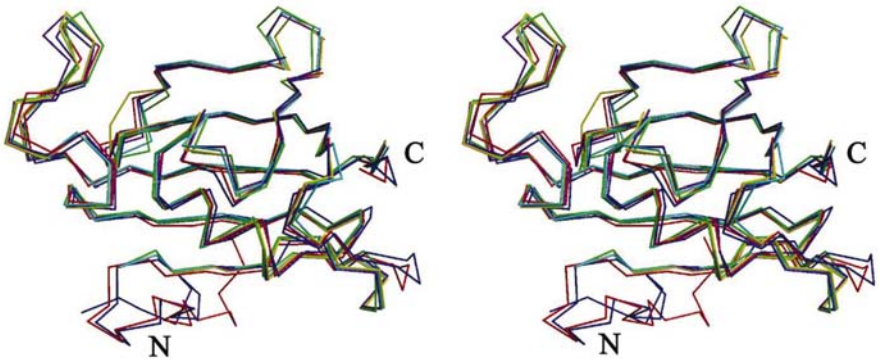

Figure 3
Superposition of the C^{α} traces of molecule *A* (red) and *B* (blue) of FKBP52-N, native FKBP12 (violet), FKBP12 complexed with FK506 and calcineurin (green), FKBP12 complexed with FK506 (cyan) and FKBP12 complexed with rapamycin (yellow).

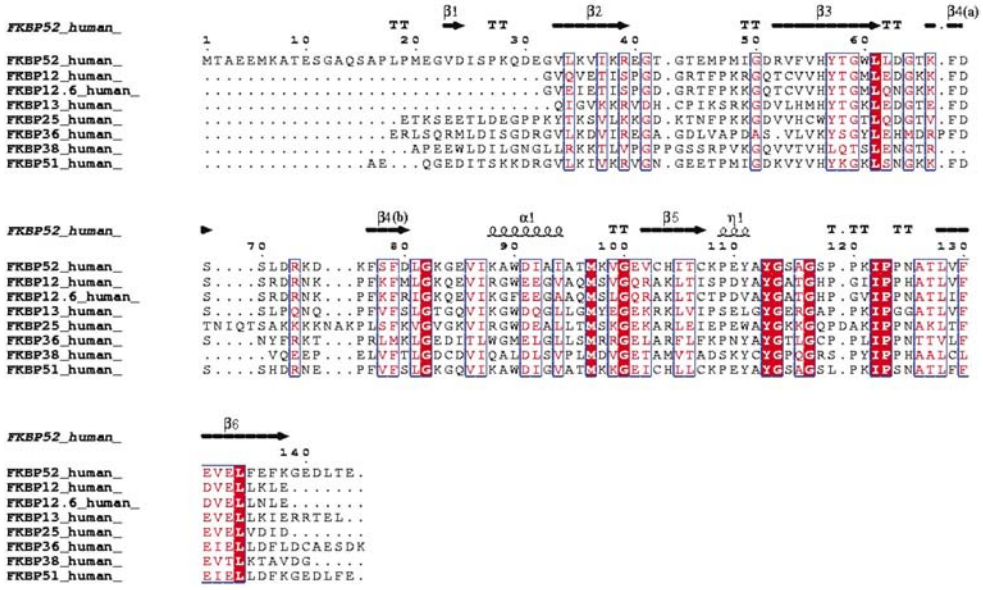

Figure 4
Sequence alignment of the sequence of the PPIase domains of human FKBPs, schematically showing the secondary structure. α1 represents an α-helix, β1–β6 represent β-strands, η1 represents a 3_{10}-helix and *T* represents a β-turn. The strictly conserved residues are shown in red boxes.

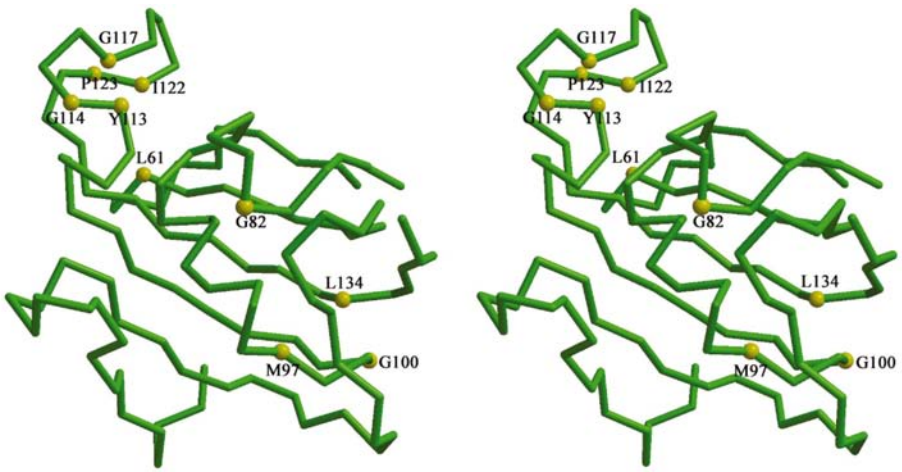

Figure 5
The locations of ten strictly conserved amino acids inthe FKBP52-N C^{α} trace.

FK506 complexed with FKBP52 or FKBP52-N does not inhibit calcineurin (Lebeau *et al.*, 1994; Yem *et al.*, 1993). Superposition of the structures of FKBP52-N and the FKBP12–FK506–calcineurin complex shows that the outstretched side chain of Lys121, which corresponds to residue Ile90 in FKBP12, would penetrate into Pro344*A* of calcineurin. This substitution destroys electrostatic and geometrical complementarity between FKBP52-N and calcineurin. A K121I mutant of FKBP52 complexed with FK506 has a high calcineurin affinity (Futer *et al.*, 1995). Thus, our structural data is consistent with this substitution being responsible for the loss of affinity for calcineurin.

3.4. Conserved amino acids

14 residues are highly conserved in FKBP12s. Of these, ten residues directly interact with bound FK506 and 12 residues interact with bound rapamycin (Kay, 1996). The corresponding 14 residues in FKBP52 are also highly conserved, except for a H118S change compared with FKBP12. The potential roles of these residues in FKBPs have been discussed previously (Kay, 1996; Van Duyne *et al.*, 1993).

Ten residues are conserved among the FK506-binding domain sequences of a number of human FKBPs (Fig. 4). In FKBP52, these residues are all located at the beginning or ends of α-helices or β-strands or in the turns, with the exception of Leu134 (Fig. 5). These positions are very important in maintaining and stabilizing the overall protein conformation. On the other hand, although about 50% of residues between FKBP52 and FKBP12 are variable, the hydrogen bonds among the main chains are strictly conserved. These hydrogen bonds play

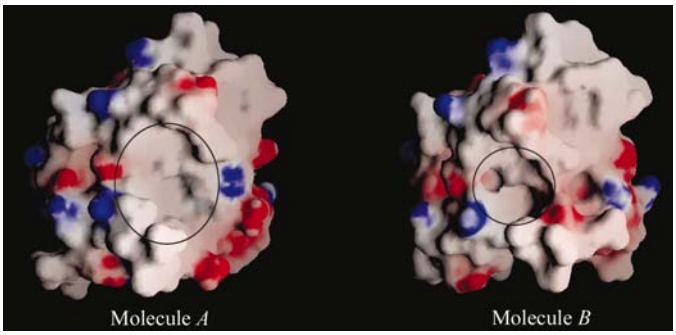

Figure 6
An additional hydrophobic patch in FKBP52-N. The circled regions represent hydrophobic patches. This figure was generated using *GRASP* (Nicholls *et al.*, 1991).

essential roles in maintaining the overall conformation of the protein. Mutational analysis has shown that the PPIase catalytic efficiency of FKBP12 is relatively insensitive to mutations at the active site (DeCenzo *et al.*, 1996; Futer *et al.*, 1995). It seems that the PPIase activity of FKBPs is determined by the overall conformation of the FK506-binding domain, especially by the overall conformation of the active site.

3.5. A potential binding site for target proteins

FKBP52-N binds to PAHX and cytoplasmic dynein; the interaction between them is increased by FK506 (Chambraud *et al.*, 1999; Galigniana *et al.*, 2001; Silverstein *et al.*, 1999). This can be explained as follows. (i) The binding sites for dynein and PAHX are different from the FK506-binding pocket; binding of FK506 can lead to a more favourable conformation for binding these target proteins. (ii) FK506 can act as a mediator between FKBP52-N and target proteins in a similar way to the action between FKBP12 and calcineurin. Analysis of the electrostatic surface of FKBP52-N revealed an additional hydrophobic patch formed by the N-terminus and β-sheets which may be a potential binding site for some ligands. Furthermore, the patch is larger and more favourable for binding a ligand in molecule *A* than in molecule *B* (Fig. 6). It is possible that this hydrophobic patch is the binding site for dynein or PAHX.

We are grateful to Luke Guddat and Mark Bartlam for their help, discussion and paper revision; we thank Hong Tang, Feng Gao and other members in our laboratory for their support. This research was supported by the following grants: NSFC Nos. 39870174 and 39970155; Project '863' No. 2001AA233011; Project '973' Nos. G1999075602, G1999011902 and 1998051105.

References

Brünger, A. T., Adams, P. D., Clore, G. M., DeLano, W. L., Gros, P., Grosse-Kunstleve, R. W., Jiang, J. S., Kuszewski, J., Nilges, M., Pannu, N. S., Read, R. J., Rice, L. M., Simonson, T. & Warren, G. L. (1998). *Acta Cryst.* D**54**, 905–921.
Callebaut, I., Renoir, J., Lebeau, M., Massol, N., Burny, A., Baulieu, E. & Mornon, J. (1992). *Proc. Natl Acad. Sci. USA*, **89**, 6270–6274.
Cameron, A. M., Steiner, J. P., Sabatini, D. M., Kaplin, A. I., Walensky, L. D. & Snyder, S. H. (1995). *Proc. Natl Acad. Sci. USA*, **92**, 1784–1788.
Chambraud, B., Radanyi, C., Camonis, J. H., Rajkowski, K., Schumacher, M. & Baulieu, E. E. (1999). *Proc. Natl Acad. Sci. USA*, **96**, 2104–2109.
Chambraud, B., Radanyi, C., Camonis, J. H., Shazand, K., Rajkowski, K. & Baulieu, E. E. (1996). *J. Biol. Chem.* **271**, 32923–32029.
Chambraud, B., Rouviere-Fourmy, N., Radanyi, C., Hsiao, K., Peattie, D. A., Livingston, D. J. & Baulieu, E. E. (1993). *Biochem. Biophys. Res. Commun.* **196**, 160–166.
Craescu, C. T., Rouviere, N., Popescu, A., Cerpolini, E., Lebeau, M. C., Baulieu, E. E. & Mispelter, J. (1996). *Biochemistry*, **35**, 11045–11052.
DeCenzo, M. T., Park, S. T., Jarrett, B. P., Aldape, R. A., Futer, O., Murcko, M. A. & Livingston, D. J. (1996). *Protein Eng.* **9**, 173–180.
Dolinski, K., Muir, S., Cardenas, M. & Heitman, J. (1997). *Proc. Natl Acad. Sci. USA*, **94**, 13093–13098.
Esnouf, R. M. (1997). *J. Mol. Graph.* **15**, 132–134.
Futer, O., DeCenzo, M. T., Aldape, R. A. & Livingston, D. J. (1995). *J. Biol. Chem.* **270**, 18935–18940.
Galat, A. (1993). *Eur. J. Biochem.* **216**, 689–707.
Galigniana, M. D., Radanyi, C., Renoir, J. M., Housley, P. R. & Pratt, W. B. (2001). *J. Biol. Chem.* **276**, 14884–14889.
Griffith, J. P., Kim, J. L., Kim, E. E., Sintchak, M. D., Thomson, J. A., Fitzgibbon, M. J., Fleming, M. A., Caron, P. R., Hsiao, K. & Navia, M. A. (1995). *Cell*, **82**, 507–522.
Jones, T. A., Zou, J. Y., Cowan, S. W. & Kjeldgaard, M. (1991). *Acta Cryst.* A**47**, 110–119.
Kay, J. E. (1996). *Biochem. J.* **314**, 361–385.
Kissinger, C. R., Parge, H. E., Knighton, D. R., Lewis, C. T., Pelletier, L. A., Tempczyk, A., Kalish, V. J., Tucker, K. D., Showalter, R. E., Moomaw, E. W., Gastinel, L. N., Habuka, N., Chen, X., Maldonado, F., Barker, J. E., Bacquet, R. & Villafranca, J. E. (1995). *Nature (London)*, **378**, 641–644.
Kraulis, P. J. (1991). *J. Appl. Cryst.* **24**, 946–950.
Laskowski, R. A., Macarthur, M. W., Moss, P. S. & Thornton, J. M. (1993). *J. Appl. Cryst.* **26**, 283–291.
Lebeau, M. C., Myagkikh, I., Rouviere-Fourmy, N., Baulieu, E. E. & Klee, C. B. (1994). *Biochem. Biophys. Res. Commun.* **203**, 750–755.
Massol, N., Lebeau, M. C., Renoir, J. M., Faber, L. E. & Baulieu, E. E. (1992). *Biochem. Biophys. Res. Commun.* **187**, 1330–1335.
Navaza, J. (1994). *Acta Cryst.* A**50**, 157–163.
Nicholls, A., Sharp, K. A. & Honig, B. (1991). *Proteins Struct. Funct. Genet.* **11**, 281–296.
Otwinowski, Z. & Minor, W. (1997). *Methods Enzymol.* **276**, 307–326.
Owens-Grillo, J. K., Czar, M. J., Hutchison, K. A., Hoffmann, K., Perdew, G. H. & Pratt, W. B. (1996). *J. Biol. Chem.* **271**, 13468–13475.
Pirkl, F., Fischer, E., Modrow, S. & Buchner, J. (2001). *J. Biol. Chem.* **276**, 37034–37041.
Pratt, W. B., Silverstein, A. M. & Galigniana, M. D. (1999). *Cell Signal.* **11**, 839–851.
Ramsey, A. J., Russell, L. C., Whitt, S. R. & Chinkers, M. (2000). *J. Biol. Chem.* **275**, 17857–17862.
Rollins, C. T., Rivera, V. M., Woolfson, D. N., Keenan, T., Hatada, M., Adams, S. E., Andrade, L. J., Yaeger, D., van Schravendijk, M. R., Holt, D. A., Gilman, M. & Clackson, T. (2000). *Proc. Natl Acad. Sci. USA*, **97**, 7096–7101.
Sanchez, E. R. (1990). *J. Biol. Chem.* **265**, 22067–22070.
Silverstein, A. M., Galigniana, M. D., Chen, M. S., Owens-Grillo, J. K., Chinkers, M. & Pratt, W. B. (1997). *J. Biol. Chem.* **272**, 16224–16230.
Silverstein, A. M., Galigniana, M. D., Kanelakis, K. C., Radanyi, C., Renoir, J. M. & Pratt, W. B. (1999). *J. Biol. Chem.* **274**, 36980–36986.
Stoddard, B. L. & Flick, K. E. (1996). *Curr. Opin. Struct. Biol.* **6**, 770–775.
Tai, P. K., Chang, H., Albers, M. W., Schreiber, S. L., Toft, D. O. &

Faber, L. E. (1993). *Biochemistry*, **32**, 8842–7.
Van Duyne, G. D., Standaert, R. F., Karplus, P. A., Schreiber, S. L. & Clardy, J. (1993). *J. Mol. Biol.* **229**, 105–124.
Wiederrecht, G., Hung, S., Chan, H. K., Marcy, A., Martin, M., Calaycay, J., Boulton, D., Sigal, N., Kincaid, R. L. & Siekierka, J. J. (1992). *J. Biol. Chem.* **267**, 21753–21760.
Wilson, K. P., Yamashita, M. M., Sintchak, M. D., Rotstein, S. H., Murcko, M. A., Boger, J., Thomson, J. A. & Navia, M. A. (1995). *Acta Cryst.* D**51**, 511–521.
Yem, A. W., Reardon, I. M., Leone, J. W., Heinrikson, R. L. & Deibel, M. R. Jr (1993). *Biochemistry*, **32**, 12571–12576.
Yem, A. W., Tomasselli, A. G., Heinrikson, R. L., Zurcher-Neely, H., Ruff, V. A., Johnson, R. A. & Deibel, M. R. Jr (1992). *J. Biol. Chem.* **267**, 2868–2871.
Young, J. C., Obermann, W. M. & Hartl, F. U. (1998). *J. Biol. Chem.* **273**, 18007–18010.